Inference of entropy production for periodically driven systems

Pedro E. Harunari ®,[1] Carlos E. Fiore ®,[2] and Andre C. Barato[3]

[1]*Complex Systems and Statistical Mechanics, Department of Physics and Materials Science,*
University of Luxembourg, L-1511 Luxembourg City, Luxembourg
[2]*Instituto de Física da Universidade de São Paulo, 05314-970 São Paulo, Brazil*
[3]*Department of Physics, University of Houston, Houston, Texas 77204, USA*

The problem of estimating entropy production from incomplete information in stochastic thermodynamics is essential for theory and experiments. Whereas a considerable amount of work has been done on this topic, arguably, most of it is restricted to the case of nonequilibrium steady states driven by a fixed thermodynamic force. Based on a recent method that has been proposed for nonequilibrium steady states, we obtain an estimate of the entropy production based on the statistics of visible transitions and their waiting times for the case of periodically driven systems. The time dependence of transition rates in periodically driven systems produces several differences in relation to steady states, which is reflected in the entropy production estimation. More specifically, we propose an estimate that does depend on the time between transitions but is independent of the specific time of the first transition, thus it does not require tracking the protocol. Formally, this elimination of the timedependence of the first transition leads to an extra term in the inequality that involves the rate of entropy production and its estimate. We analyze a simple model of a molecular pump to understand the relation between the performance of the method and physical quantities such as energies, energy barriers, and thermodynamic affinity. Our results with this model indicate that the emergence of net motion in the form of a probability current in the space of states is a necessary condition for a relevant estimate of the rate of entropy production.

I. INTRODUCTION

Stochastic thermodynamics [1–3] is a modern theoretical framework that generalizes thermodynamics to systems that can be small, i.e., made of only a few degrees of freedom, and out of equilibrium. The success of this theory is also due to the fact that such small systems have become accessible in experiments. Examples include single molecules such as molecular motors, colloids and quantum dots [4]. A main observable of interest in stochastic thermodynamics is the rate of entropy production, which quantifies the thermodynamic cost of an out-of-equilibrium system.

It is often the case in an experiment that not all states of the mesoscopic system are accessible. Therefore, the inference of properties of the system, such as its rate of entropy production, from partial information is a fundamental theoretical problem in stochastic thermodynamics. In particular, while well-controlled experiments with full information about the system have provided beautiful connections between modern theory and experiments [5–10], connecting stochastic thermodynamics with less-controlled experiments in molecular biophysics remains a major challenge, which is closely related to the problem of inferring properties of the system from partial information.

Much work on the problem of inferring the entropy production and related observables has been done. The thermodynamic uncertainty relation [11–13] has been used to infer entropy production and related observables from the fluctuations of a current [14–19]. The rate of entropy production can also be estimated from the Kullback-Leibler divergence between the probability of a coarse-grained trajectory and the probability of the respective reversed trajectory [20–23]. Another approach to estimating the entropy production is to assume that the visible dynamics correspond to a hidden Markov process and use the observable data to infer the underlying Markov process [24–26]. More generally, the related topic of coarse graining in stochastic thermodynamics has been widely studied [27–36]. Most of these works on the estimation of entropy production are suitable for steady states, however, some works have recently addressed time-dependent cases [37–41].

Particularly important for this work is a method to estimate the rate of the entropy production from the statistics of the sequences and times between a few visible transitions proposed independently in two recent papers [42,43]. This approach is promising as it is reasonable to expect that the statistics of the time between transitions, i.e., the intertransition time, is accessible in an experiment. These two references concentrate on systems in nonequilibrium steady states, which are driven by constant thermodynamic forces.

In contrast to nonequilibrium steady states, periodically driven systems are driven by an external periodic protocol. Examples of periodically driven systems include cyclic heat engines [44–49] and artificial molecular machines [50–58]. It is known that periodically driven systems and nonequilibrium steady states can display substantial differences [59,60], therefore, the inference method for steady states from [42,43] prompts the following questions. How is the method extended to periodically driven systems? What are the differences in the

application of the method between steady states and periodically driven systems?

In this paper, we provide answers to these questions. We show that the rate of entropy production can be inferred from the statistics of sequences and intertransition times between a few visible transitions in periodically driven systems. We find several important differences in relation to steady states. Since transition rates are time-dependent, the statistics of transition pairs depend on the intertransition time and the initial time of the first transition. We overcome this issue by developing an estimator that only depends on the intertransition time. The formal elimination of this dependence on the time of the first transition leads to an inequality between the estimator and the real rate of entropy production that contains an extra term. We also find an estimator that depends on both the intertransition time and the time of the first transition. Even though this bound provides a better estimate of the rate of entropy production, compared to the one that only depends on intertransition times, in practice, it requires one histogram of intertransition times per each considered initial time, which can be computationally expensive.

The estimator of the entropy production involves two different distributions of the intertransition time, one associated with the original forward protocol and the other associated with the time-reversed protocol. This is in contrast to steady states that only involve one distribution. Hence, the application of the method requires two experiments, one with the forward protocol and another with the time-reversed protocol.

A simple three-state model with time-dependent energies and energy barriers [61] is used as a proof of concept. We obtain the following results with this model. First, for a unicyclic network of states, while a similar method gives the exact value of the entropy production for steady states [42,43], our estimate only provides a lower bound on the rate of entropy production for periodically driven systems. Second, in contrast to steady states, periodically driven systems can have entropy production in the absence of a net current in the space of states. For this case of absence of net motion, the estimator for entropy production gives a numerical result compatible with zero, which suggests that net motion is an essential feature for our estimator to provide information about the rate of entropy production.

An analytical procedure to calculate the distribution of the probability density of the intertransition time for steady states was introduced in [42,43,62]. This procedure maps the problem of calculating the intertransition time distribution into the problem of calculating the time-dependent probability of an absorbing state of a certain auxiliary process. We generalize this procedure to a periodically driven system, providing a pathway to obtain our estimator analytically.

The paper is organized as follows. In Sec. II, we introduce the key quantities analyzed here and define the three-state model. Our numerical results showing the application of the method to the specific model are shown in Sec. III. The inequality that involves the rate of entropy production, its estimator, and an extra term is proved in Sec. IV. The analytical method to determine the intertransition time distribution is discussed in Sec. V. We conclude in Sec. VI.
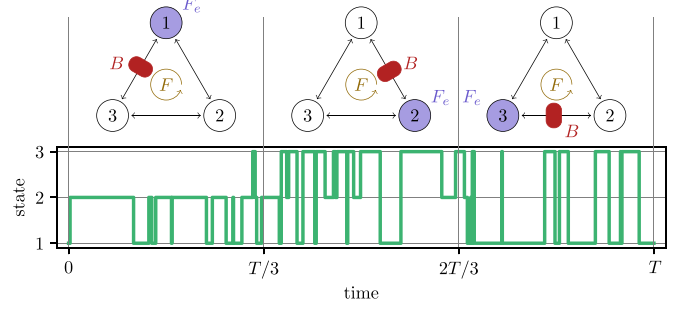

FIG. 1. Upper panel: periodic protocol for the three-state model. The energy F_e and the energy barrier B rotate clockwise in each third part of the period. Lower panel: example of a stochastic trajectory with transitions between states and waiting times.

II. OBSERVABLE TRANSITIONS, INTERTRANSITION TIME STATISTICS AND INFERENCE OF ENTROPY PRODUCTION

A. Markov processes with time-periodic transition rates

Here, we consider Markov processes with a finite number of discrete states denoted by i and j. The time-dependent transition rate from state i to state j is denoted $w_{ij}(t)$. This transition rate is time periodic with period T, i.e., $w_{ij}(t) = w_{ij}(t + T)$. The probability to be in state i at time t is written as $P_i(t)$ and follows the master equation

$$\frac{d}{dt}P_i(t) = \sum_{j \neq i}[P_j(t)w_{ji}(t) - P_i(t)w_{ij}(t)]. \quad (1)$$

We are interested in the long time limit $t \to \infty$, for which the distribution $P_i(t)$ becomes time periodic with period T. This long-time limit solution of the master equation is denoted by $P_i(t)$ for the remainder of this paper. In stochastic thermodynamics, we restrict to rates with the property that if $w_{ij}(t) \neq 0$ then $w_{ji}(t) \neq 0$.

The rate of entropy production is given by [2]

$$\sigma \equiv \frac{1}{T}\int_0^T dt \sum_{i,j} P_i(t)w_{ij}(t) \ln \frac{w_{ij}(t)}{w_{ji}(t)}. \quad (2)$$

This physical quantity can be expressed as the sum of terms that are a product of thermodynamic flux and the respective thermodynamic affinity with the use of the generalized detailed balance relation [46,61]. We discuss this expression for the entropy production for the particular model we introduce in the following section.

B. Model definition

As a proof of concept, we consider the following model for a molecular pump depicted in Fig. 1. A similar model, with a stochastic protocol instead of the deterministic protocol considered here, has been analyzed in [61]. The model has three states, which we label as $i = 1, 2, 3$. There is one energy F_e and one energy barrier B, while the remaining energies and energy barriers are zero. The periodic protocol is piecewise, with the period divided into three parts. For the first part, corresponding to $0 < t < T/3$, the energy of state 1 is $E_1(t) = F_e$ and the energy barrier between states 3 and 1 is $B_{31}(t) = B$.

The other two energies and two energy barriers are 0. For the second part, corresponding to $T/3 < t < 2T/3$, $E_2(t) = F_e$, and $B_{12}(t) = B$, and the other energies and energy barriers are zero. For the third part, corresponding to $2T/3 < t < T$, $E_3(t) = F_e$, and $B_{23}(t) = B$, and the other energies and energy barriers are zero.

Here, we set Boltzmann's constant and temperature to $k_B = T = 1$, where T represents temperature and not period only in this equation, throughout. The transition rates for this model are given by

$$w_{ii+1}(t) = k e^{E_i(t) - B_{ii+1}(t)}, \qquad (3)$$

and

$$w_{i+1i}(t) = k e^{E_{i+1}(t) - B_{ii+1}(t)}. \qquad (4)$$

Due to periodic boundary conditions, for $i=3$, we set $i+1 = 1$. The parameter k sets the speed of the rates.

We now discuss the sources of entropy production in this model. Work is exerted on the system due to the time dependence of the energies. The entropy production is equal to the average work and can be written as

$$\sigma = F_e J_e, \qquad (5)$$

$$J_e = \frac{1}{T} \sum_{i=1}^{3} [P_{i+1}(iT/3) - P_i(iT/3)]. \qquad (6)$$

This expression for σ is equivalent to Eq. (2) [61]. It can be understood as follows. Let us consider the term $i = 1$ in the summation, corresponding to the time $T/3$ of the protocol. At this time if the system is at state 1, with probability $P_1(T/3)$, it will lose an energy F_e since the energy of the system changes from F_e to 0. If the system is at state 2, with probability $P_2(T/3)$, it will gain an energy F_e. The same reasoning applies to $i = 2$ and $i = 3$.

The energy barrier B does not appear in the expression for σ explicitly. It appears only implicitly as it affects the probabilities $P_i(t)$. Even if $B = 0$, the rate of entropy production can be nonzero. However, an energy barrier B is a necessary condition to create net motion in the clockwise direction, as explained in the literature on "no-pumping theorems" [50–52]. This net motion is quantified by the average current

$$J = \frac{1}{T} \int_0^T dt \sum_{i=1}^{3} \frac{J_{ii+1}(t)}{3}. \qquad (7)$$

In other words, when $B = 0$, J also vanishes. However, even with $J = 0$, the periodically driven system remains out of equilibrium when $Fe \neq 0$, resulting in positive entropy production. This behavior contrasts sharply with steady-state systems, where nonzero entropy production is always associated with currents. As shown below, the presence of this net motion quantified by J in periodically driven systems is essential for our estimate of the rate of the entropy production. If $J = 0$ our estimate is much smaller than the entropy production in general, providing little to no information.

We also consider the case of the presence of a fixed thermodynamic affinity F that would drive the system to a nonequilibrium steady state in the absence of a periodic protocol. The transition rates are modified to

$$w_{ii+1}(t) = k e^{E_i(t) - B_{ii+1}(t) - F/3}, \qquad (8)$$

and

$$w_{i+1i}(t) = k e^{E_{i+1}(t) - B_{ii+1}(t)}, \qquad (9)$$

where the negative sign in $-F/3$ in the first equation implies that a positive F leads to a force in the counter-clockwise direction.

In the presence of this fixed affinity F the entropy production in Eq. (2) becomes

$$\sigma = F_e J_e - F J, \qquad (10)$$

where J is the current in Eq. (7). This general expression for the entropy production in terms of currents J_e and J and affinities F and F_e has been obtained in [61]. The minus sign in the term FJ comes from the fact that F points in the counterclockwise direction and J points in the clockwise direction.

This model can also operate as an engine when the term $F_e J_e$ is positive and the term $-F J$ is negative. In this regime F_e together with the energy barrier B creates a clockwise current that does work against the counterclockwise force F [53,61]. We also analyze the estimator of the entropy production in this regime.

C. Intertransition time

An example of a stochastic trajectory is shown in Fig. 1. This trajectory is a sequence of transitions and waiting times between transitions. We denote a jump, or transition, from state i to state j as $\ell = ij$. The reversed jump from j to i is denoted by $\bar{\ell}$. The set of visible transitions is denoted by $\mathcal{L}$. For instance, for the three-state model, we have a total of six possible transitions, two between each pair of states. If we only have access to the two transitions between the pair of states 1 and 2, then two of the six transitions are part of the set $\mathcal{L}$.

The distribution $\mathcal{P}_{\ell', \tau + t_0 | \ell, t_0}$ is the probability density that a transition ℓ' occurs at time $\tau + t_0$ given that transition ℓ occurred at the initial time t_0 and that no other visible transition in $\mathcal{L}$ occurs before $\tau + t_0$, where τ is the intertransition time. This dependence on the time of the first transition t_0 is a consequence of the time-dependent transition rates. An important fact about $\mathcal{P}_{\ell', \tau + t_0 | \ell, t_0}$ is its dependence on the set of visible transitions $\mathcal{L}$, which is illustrated in Fig. 2 for a particular example. In this figure, there are three transitions and two intertransition times if only the transitions between states 1 and 2 are visible and there are four transitions and three intertransition times if the transitions between states 2 and 3 are also part of $\mathcal{L}$. To simplify notation we do not write this dependence explicitly in $\mathcal{P}_{\ell', \tau + t_0 | \ell, t_0}$.

Our objective here is to infer the rate of entropy production from sequences and intertransition time statistics of a few visible transitions. Calculating the histogram associated with $\mathcal{P}_{\ell', \tau + t_0 | \ell, t_0}$ from a trajectory can be a hard task since it depends on the intertransition time τ and the initial time t_0. A more practical method would be to only keep track of the intertransition times in the trajectory, without keeping track of the time for the first transition. In practice, if we only keep
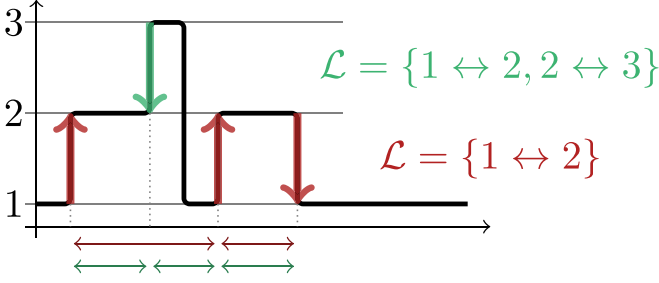
FIG. 2. Sequence of intertransition times for $\mathcal{L} = \{1 \to 2, 2 \to 1\}$ and for $\mathcal{L} = \{1 \to 2, 2 \to 1, 2 \to 3, 3 \to 2\}$. For this particular trajectory, there are two intertransition times for the first case and three intertransition times for the second case.

track of the intertransition times, we will average out over all possible initial times t_0. This average is over the probability $\mathcal{P}_{t_0|\ell}$, which is the conditional probability density of sampling time $t_0 \in [0, T]$ given that transition ℓ occurred. Based on this reasoning we consider the quantity

$$\psi_{\ell'|\ell}(\tau) \equiv T^{-1} \int_0^T dt_0 \mathcal{P}_{\ell', \tau + t_0|\ell, t_0} \mathcal{P}_{t_0|\ell}. \quad (11)$$

In other words, the quantity $\psi_{\ell'|\ell}(\tau)$ is particularly convenient from a practical perspective. If we simply count the number of transitions within a certain time interval for the pair $\ell'|\ell$ in a trajectory, without accounting for the initial time of the first transition, we obtain the histogram associated with $\psi_{\ell'|\ell}(\tau)$.

The conditional probability density $\mathcal{P}_{t_0|\ell}$ can be written in terms of the transition rates $w_{ij}(t_0)$ and the long time limit probability $P_i(t_0)$ that is the solution of the master equation. If we denote $\ell = ij$, then

$$\mathcal{P}_{t_0|\ell} = \frac{P_i(t_0) w_{ij}(t_0)}{\int_0^T dt_0 P_i(t_0) w_{ij}(t_0)}. \quad (12)$$

In Sec. V we provide a method to calculate $\mathcal{P}_{\ell', \tau + t_0|\ell, t_0}$ and, consequently, $\psi_{\ell'|\ell}(\tau)$ analytically.

D. Reversed protocol

In order to estimate the entropy production from a few visible transitions in periodically driven systems we also need the statistics of the intertransition time associated with the reversed protocol. The mathematical definition for the reversed protocol is given by the following equation for the transition rates:

$$w_{ij}^\dagger(t_0) \equiv w_{ij}(T - t_0). \quad (13)$$

Physically, for the model in Fig. 1, the reversed protocol corresponds to the sequence of pictures showing the position of the energy and energy barrier in reverse order.

In order to calculate the probability density for the intertransition time associated with the reversed protocol $\psi_{\ell'|\ell}^\dagger(\tau)$, we also need to generate a trajectory with the reversed protocol. From a practical perspective, in order to estimate the rate of entropy production with our method there is a need to generate trajectories from two experiments, one with the forward protocol and another with the backward protocol.

E. Inference of entropy production from the statistics of the intertransition time

Our estimator for average rate of entropy production σ is given by

$$\hat{\sigma} = K \sum_{\ell, \ell' \in \mathcal{L}} \int_0^\infty dt \, \psi_{\ell'|\ell}(\tau) \mathcal{P}_\ell \ln \frac{\psi_{\ell'|\ell}(\tau)}{\psi_{\bar{\ell}|\bar{\ell'}}^\dagger(\tau)}, \quad (14)$$

where the activity K is the average number of visible transitions in $\mathcal{L}$ per time and P_ℓ is the probability that an observable transition is ℓ, irrespective of the time of its occurrence. These quantities, K and $\mathcal{P}_\ell$, can be written in terms of the long-time solution of the master equation $P_i(t_0)$, they are given by

$$K = T^{-1} \int_0^T dt_0 \sum_{ij \in \mathcal{L}} P_i(t_0) w_{ij}(t_0), \quad (15)$$

and

$$\mathcal{P}_\ell = K^{-1} T^{-1} \int_0^T dt_0 P_i(t_0) w_{ij}(t_0), \quad (16)$$

where $\ell = ij$. We can obtain this estimate from a trajectory (and a second trajectory with the reversed protocol) where we can only observe a few visible transitions and the intertransition times. The activity K is evaluated by simply counting the total number of transitions and dividing by the total time, $\mathcal{P}_\ell$ can be obtained by counting the number of transitions ℓ and dividing by the total number of transitions, $\psi_{\ell'|\ell}(\tau)$ can be obtained from a histogram of the intertransition times from the trajectory, and, finally, $\psi_{\bar{\ell}|\bar{\ell'}}^\dagger(\tau)$ can be similarly obtained with the only difference that the reverse protocol is applied.

III. RESULTS FOR CASE STUDY

In this section, we show our numerical study of entropy production and the estimator for the model defined in Sec. II B. We observed the estimate $\hat{\sigma}$ below the real rate of entropy production σ in all our numerical results within this model. However, the formal inequality connecting both quantities contains an extra term X and reads $\sigma \geqslant \hat{\sigma} - X$, where the extra term fulfills $X \geqslant 0$. This inequality is proved in the next section. In Figs. 3 and 4, we also illustrate it by plotting $\hat{\sigma} - X$, which can be negative.

The numerical results shown in the figures in this section were obtained via Monte Carlo simulation with discretized time, where the time step, which is much shorter than the characteristic time of the fastest jump, is small enough such that no relevant difference is observed by taking a smaller time step. The statistics of sequences of visible jumps and their intertransition times were obtained by analyzing their frequency from long enough trajectories such that the empirically measured quantities presented reasonable convergence. The parameter k, which sets the time scale of the transition rates in Eqs. (8) and (9), and the period T are set to $k = 10$ and $T = 1$. We here consider that only the transitions between states 1 and 2 are visible, i.e., $\mathcal{L} = \{1 \to 2, 2 \to 1\}$.

A. Energy, energy barrier, and entropy production estimate

In Fig. 3, we show results for the fixed external affinity $F = 0$. In Fig. 3(a), the energy barrier is $B = 0$, which leads
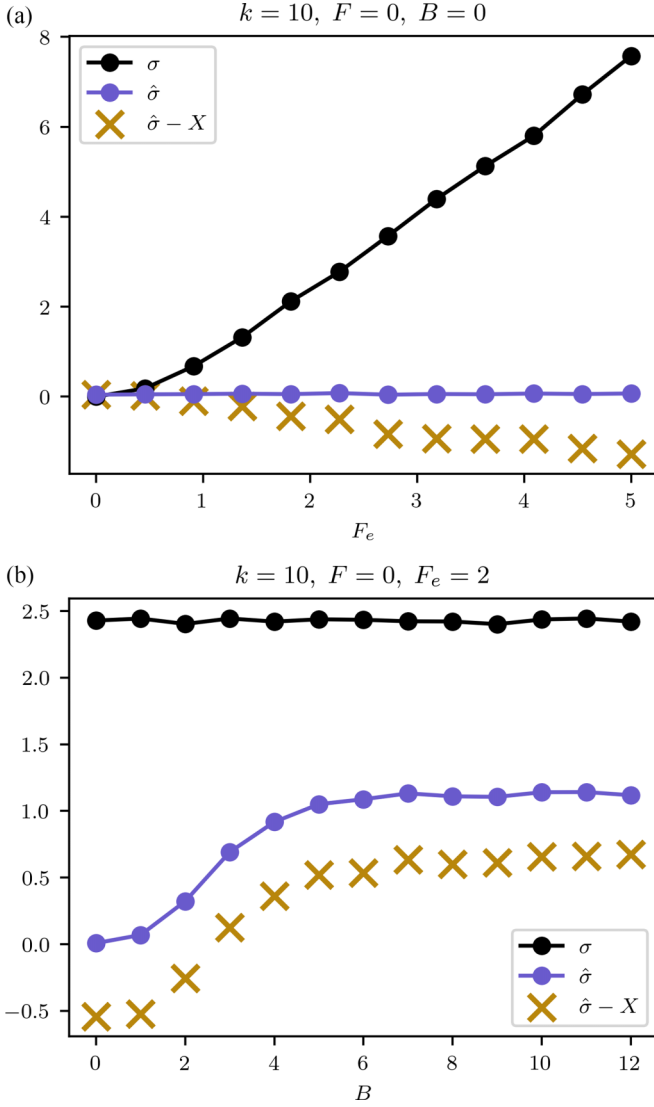
FIG. 3. Entropy production σ, its estimate $\hat{\sigma}$, and its lower bound $\hat{\sigma} - X$ as functions of (a) the energy F_e for $B = 0$ and (b) the energy barrier B for $F_e = 2$.
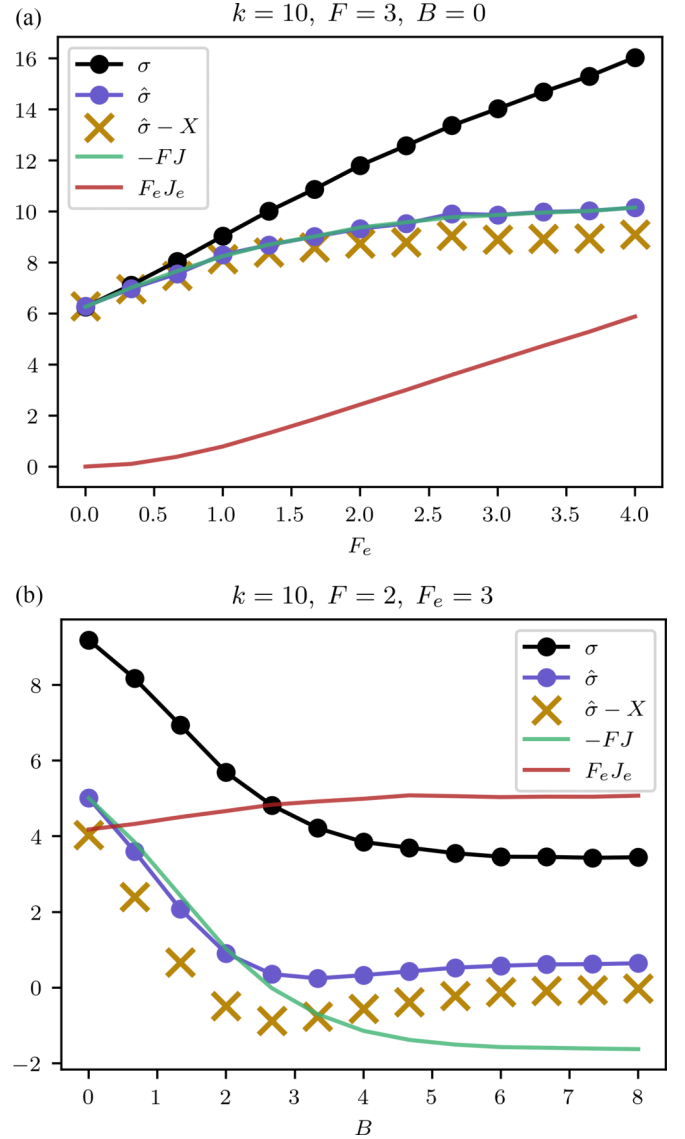

FIG. 4. Entropy production $\sigma = FJ + F_e J_e$, its estimate $\hat{\sigma}$, and its lower bound $\hat{\sigma} - X$ as functions of (a) the energy F_e for $B = 0$ and (b) the energy barrier B for $F_e = 3$.

to a net current $J = 0$, as discussed in Sec. II. Even though the current J does not appear in the formula for σ in Eq. (10), it seems to play a fundamental role for the estimate $\hat{\sigma}$. For $B = 0$, we see that the estimate $\hat{\sigma}$ is numerically compatible with 0 and, therefore, does not provide any useful information about the rate of entropy production σ. Hence, the emergence of a current J, which is not necessary for a nonzero entropy production σ in periodically driven systems, seems to be a necessary condition for a meaningful estimate $\hat{\sigma}$.

The case of a nonzero energy barrier is shown in Fig. 3(b). Here, we see that the estimate $\hat{\sigma}$ is nonzero for $B > 0$ that leads to the emergence of a nonzero current J. From the results in Fig. 3, we observe that even for unicyclic networks the estimate $\hat{\sigma}$ is not equal to the entropy production σ. This situation is in contrast to steady states, where a similar estimate becomes equal to the entropy production for unicyclic networks [42,43].

In summary, our results for the case of $F = 0$ lead to two main conclusions. First, it seems that the emergence of a current J is a relevant condition for the usefulness of $\hat{\sigma}$ as an estimator. Second, even in a unicyclic network, the estimate $\hat{\sigma}$ is not equal to the exact rate of entropy production σ.

B. Role of external fixed affinity F

We now consider the case of a nonzero fixed affinity F. In Fig. 4(a), we compare the estimate $\hat{\sigma}$ for the energy barrier $B = 0$ with the rate of entropy production σ, and its two contributions in Eq. (10). As we can see in the figure, $\hat{\sigma}$ seems to follow the term $-FJ$ and does not capture much information about the contribution due to the work term $J_e F_e$, reinforcing the connection between the estimator and the net current.

In Fig. 4(b), we show our results for $B \neq 0$. Here, we can see that the estimate $\hat{\sigma}$ is sensitive to the work term $J_e F_e$, even

in the regime where $-JF$ becomes negative. In this regime, the system operates as an engine with work exerted against the internal force F. Therefore, the results in Fig. 4, together with the need for net motion, suggest that the presence of energy barriers seems to be a necessary condition for the estimate $\hat{\sigma}$ to capture information on the work term $F_e J_e$ of the rate of entropy production σ.

IV. PROOF OF THE BOUND AND THE EMERGENCE OF THE EXTRA TERM

A. First bound $\sigma_{\mathcal{L}}$

A full trajectory of the Markov process with all transitions visible is denoted by γ_{t_f}, where t_f is the total time of the trajectory. We are interested in the limit $t_f \to \infty$. The rate of entropy production is given by the relative entropy between the probability of a trajectory $P[\gamma_{t_f}]$ and its time reverse under reversed protocol $P^\dagger[\gamma_{t_f}^\dagger]$ [2], where the superscript in $P^\dagger$ means the probability associated with the reversed protocol and the superscript in $\gamma_{t_f}^\dagger$ means the reverse of the trajectory γ_{t_f}. This formula is written as

$$\sigma = \lim_{t_f \to \infty} \frac{1}{t_f} \sum_{\gamma_{t_f}} P[\gamma_{t_f}] \ln \frac{P[\gamma_{t_f}]}{P^\dagger[\gamma_{t_f}^\dagger]}. \tag{17}$$

Formally, the sum over all trajectories $\sum_{\gamma_{t_f}}$ corresponds to a functional integration.

Let θ be a coarse-graining map such that $\Gamma_{t_f} = \theta \gamma_{t_f}$, it can represent arbitrary coarse graining. Here, we consider the removal of hidden transitions and only a subset of transitions $\mathcal{L}$ remain visible. This map is noninjective (many-to-one) since the trajectory details are contracted, thus many full trajectories γ_{t_f} can give rise to the same coarse-grained trajectory Γ_{t_f}. For the probability of the coarse-grained trajectory Γ, we can write

$$P[\Gamma] = \sum_{\gamma \in \theta^{-1}\Gamma} P[\gamma]. \tag{18}$$

We consider a time-reversal operation that commutes with the coarse-graining map, $(\theta\gamma)^\dagger = \theta(\gamma^\dagger) =: \Gamma^\dagger$, which is achieved by noticing that transitions ℓ are replaced by $\bar{\ell}$ in the time-reversed trajectory. A lower bound on entropy production rate σ, accessible from the statistics of the visible transition that pertain to $\mathcal{L}$, is defined as

$$\sigma_{\mathcal{L}} \equiv \lim_{t_f \to \infty} \frac{1}{t_f} \sum_{\Gamma_{t_f}} P[\Gamma_{t_f}] \ln \frac{P[\Gamma_{t_f}]}{P^\dagger[\Gamma_{t_f}^\dagger]}, \tag{19}$$

which fulfills

$$\sigma \geqslant \sigma_{\mathcal{L}}, \tag{20}$$

due to the log-sum inequality.

The coarse-grained trajectory Γ_{t_f} is a sequence of visible transitions $\ell_i \in \mathcal{L}$ that take place at times t_i. If the trajectory has N visible transitions then $i = 1, 2, \ldots, N$. The probability of a given trajectory Γ reads

$$P[\Gamma] = \mathcal{P}_{\ell_1, t_1} \prod_{i=2}^{N} \mathcal{P}_{\ell_i, t_i | \ell_{i-1}, t_{i-1}}, \tag{21}$$
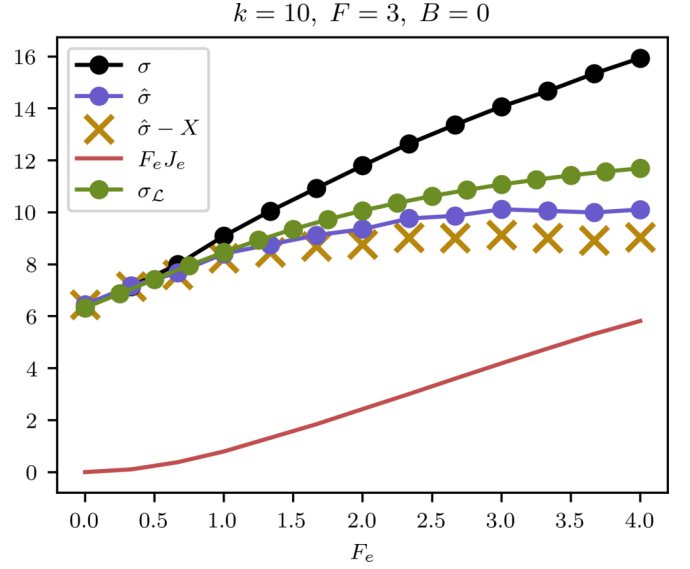

FIG. 5. The quantities of Fig. 4(a) and $\sigma_{\mathcal{L}}$.

where $\mathcal{P}_{\ell_i, t_i | \ell_{i-1}, t_{i-1}}$ is the conditional probability of transition ℓ_i being observed at t_i given that transition ℓ_{i-1} occurred at t_{i-1}, provided no other visible transitions in $\mathcal{L}$ occurred in between. A similar expression is valid for $P^\dagger[\Gamma^\dagger]$, which is

$$P^\dagger[\Gamma^\dagger] = \mathcal{P}^\dagger_{\bar{\ell}_N, t_f - t_N} \prod_{i=0}^{N-2} \mathcal{P}^\dagger_{\bar{\ell}_{N-i-1}, t_f - t_{N-i-1} | \bar{\ell}_{N-i}, t_f - t_{N-i}}. \tag{22}$$

Even though we are interested only in the limit of $t_f \to \infty$, these two expressions for the probability of a trajectory are valid for any finite t_f.

We now obtain an expression for the lower bound on the entropy production in Eq. (19) using the expressions for the probability of a trajectory in Eq. (21) and in Eq. (22), which reads

$$\sigma_{\mathcal{L}} = \lim_{t_f \to \infty} \frac{K}{t_f} \sum_{\ell', \ell \in \mathcal{L}} \int_t^{t_f} dt' \int_0^{t_f} dt \, \mathcal{P}_{\ell', t'; \ell, t} \ln \frac{\mathcal{P}_{\ell', t' | \ell, t}}{\mathcal{P}^\dagger_{\bar{\ell}, t_f - t | \bar{\ell}', t_f - t'}}, \tag{23}$$

where $\mathcal{P}_{\ell', t'; \ell, t} = \mathcal{P}_{\ell', t' | \ell, t} \mathcal{P}_{\ell, t}$ is the joint distribution. In this expression, since we are considering the limit $t_f \to \infty$, the contribution of the boundary term in $\ln(P[\Gamma_{t_f}]/P^\dagger[\Gamma_{t_f}^\dagger])$, which is $\ln(\mathcal{P}_{\ell_1, t_1}/\mathcal{P}^\dagger_{\bar{\ell}_N, t_f - t_N})$, goes to zero.

The expression in (23) can be further simplified for a time-periodic system with period T. This simplification reads

$$\sigma_{\mathcal{L}} = \frac{K}{T} \sum_{\ell', \ell \in \mathcal{L}} \int_0^\infty d\tau \int_0^T dt_0 \, \mathcal{P}_{\ell', \tau + t_0; \ell, t_0} \ln \frac{\mathcal{P}_{\ell', \tau + t_0 | \ell, t_0}}{\mathcal{P}^\dagger_{\bar{\ell}, \tau + t_0^* | \bar{\ell}', t_0^*}}, \tag{24}$$

where $t_0^* = T - [(\tau + t_0) \mod T]$. In Fig. 5 we show that $\sigma_{\mathcal{L}}$ can provide a better estimate of σ in comparison to $\hat{\sigma}$, where $\sigma_{\mathcal{L}}$ was calculated using the analytical methods of Sec. V. However, in practice, it is much more difficult to obtain this estimator from a trajectory generated in a simulation or experiment. The main difference is that, for each pair of transitions,

this quantity requires one histogram for each initial time t_0 in the period, while $\hat{\sigma}$ uses only one histogram.

B. Elimination of t_0

The estimate $\hat{\sigma}$, that only depends on the intertransition times, arises from the use of a log-sum inequality in t_0. The extra term is defined as

$$X \equiv \frac{K}{T} \sum_{\ell',\ell \in \mathcal{L}} \int_0^\infty \mathrm{d}\tau \int_0^T \mathrm{d}t_0 P_{\ell',\tau+t_0;\ell,t_0} \ln \frac{P_{t_0|\ell}}{P_{t_0^*|\ell'}^\dagger} \geqslant 0. \quad (25)$$

From this definition of X and (24), using the log-sum inequality in t_0 we obtain

$$\sigma_{\mathcal{L}} + X \geqslant \hat{\sigma}, \quad (26)$$

where $\hat{\sigma}$ is our estimate given by Eq. (14). Since $\sigma \geqslant \sigma_{\mathcal{L}}$ we obtain

$$\sigma \geqslant \hat{\sigma} - X. \quad (27)$$

The extra term X fulfills the inequality

$$X \geqslant 0, \quad (28)$$

which is obtained from Eqs. (12) and (25), and the log-sum inequality in t_0. The term X can be calculated from a trajectory (and another one with the reversed protocol) in the following way. First, we obtain the distributions $\mathcal{P}_{t_0|\ell}$ from a trajectory with forward protocol and $\mathcal{P}_{t_0|\ell}^\dagger$ from a trajectory with the reversed protocol. Then, we can run over all transitions in a visible trajectory Γ with forward protocol, with its probability represented in Eq. (21), and compute $\ln(\mathcal{P}_{t_i|\ell_i}/P_{t_f-t_i|\bar{\ell}_i}^\dagger)$ whenever a visible transition ℓ_i happens at time t_i. If the probabilities are empirically inferred from the same trajectory, correlations can give rise to convergence issues, thus it is better to use independent trajectories. Note that there is no need to calculate a distribution that depends on two times in order to calculate X from a trajectory, which was a main practical issue with the tighter estimate $\sigma_{\mathcal{L}}$.

In summary, our estimate $\hat{\sigma}$ is not connected to σ by a formal inequality to our knowledge. However, within our numerics restricted to one case study $\hat{\sigma}$ is below σ. This evidence is not enough to make a conjecture but it leaves the possibility of an inequality open. If we consider $\hat{\sigma} - X$ as an estimate, then we do have a formal inequality.

V. ANALYTICAL METHOD TO DETERMINE THE INTERTRANSITION TIME DISTRIBUTION

Our estimator $\hat{\sigma}$ depends on the intertransition time probability density $\psi_{\ell'|\ell}(\tau)$, which can be obtained from histograms of observable trajectories. We show how to calculate this distribution analytically for a periodically driven system. Similar to a procedure for steady states from [42,43,62], we map the problem of determining $\psi_{\ell'|\ell}(\tau)$ onto a survival probability problem of an auxiliary Markov process with absorbing states. The difference here is that the transition rates are time dependent, which makes the procedure more involved.

The formal solution of the master equation (1) is

$$P_i(t) = \sum_j \left[\mathcal{T}\left\{ \exp \int_{t_0}^t \mathrm{d}s \mathbf{W}(s) \right\} \right]_{j,i} P_j^{\mathrm{ini}}(t_0), \quad (29)$$

where t_0 is the initial time, P^{ini} the initial distribution, and $\mathcal{T}\{\exp \bullet\}$ denotes the time-ordered matrix exponential. The stochastic matrix $\mathbf{W}(t)$ has elements $[\mathbf{W}(s)]_{ij} = w_{ji}(s)$ for $i \neq j$ and $[\mathbf{W}(s)]_{ii} = -\sum_j \omega_{ij}(s)$. The long time solution $P_i(t)$ of the master equation can be obtained with Floquet theory [63].

To calculate the intertransition time distribution $\psi_{\ell'|\ell}(t)$ we define an auxiliary process that has absorbing states. This auxiliary process has an extra number of states that equals the number of transitions in $\mathcal{L}$, the set of visible transitions. All extra states are absorbing. For instance, if the transition $\ell = 1 \rightarrow 2 \in \mathcal{L}$ then the transition from 1 to 2 does not go to state 2 in this new auxiliary process. Instead, it goes to a new absorbing state denoted $\ell = 1 \rightarrow 2$. The stochastic matrix associated with this auxiliary process is denoted $\mathbf{W}_{\mathrm{aux}}(t)$.

As an example, we consider the three-state model. The stochastic matrix associated with the original process reads

$$\mathbf{W}(t) = \begin{bmatrix} -r_1(t) & w_{21}(t) & w_{31}(t) \\ w_{12}(t) & -r_2(t) & w_{32}(t) \\ w_{13}(t) & w_{23}(t) & -r_3(t) \end{bmatrix}, \quad (30)$$

where $r_i(t) = \sum_j w_{ij}(t)$. For $\mathcal{L} = \{1 \rightarrow 2, 2 \rightarrow 1\}$, the stochastic matrix for the auxiliary process reads

$$\mathbf{W}_{\mathrm{aux}}(t) = \begin{bmatrix} -r_1(t) & 0 & w_{31}(t) & 0 & 0 \\ 0 & -r_2(t) & w_{32}(t) & 0 & 0 \\ w_{13}(t) & w_{23}(t) & -r_3(t) & 0 & 0 \\ 0 & w_{21}(t) & 0 & 0 & 0 \\ w_{12}(t) & 0 & 0 & 0 & 0 \end{bmatrix}, \quad (31)$$

where the fourth state is associated with $2 \rightarrow 1$ and the fifth state is associated with $1 \rightarrow 2$.

The conditional distribution $\mathcal{P}_{\ell',\tau+t_0|\ell,t_0}$ is related to the time-dependent solution of this auxiliary process. Let's denote a generic state of the auxiliary process by a. The probability of being in state a at time t is denoted by $Q_a(t)$. The condition that ℓ and t_0 are given in the conditional probability $\mathcal{P}_{\ell',\tau+t_0|\ell,t_0}$ is reflected in the initial probability of this auxiliary process. The time for the transition rates for this initial condition is

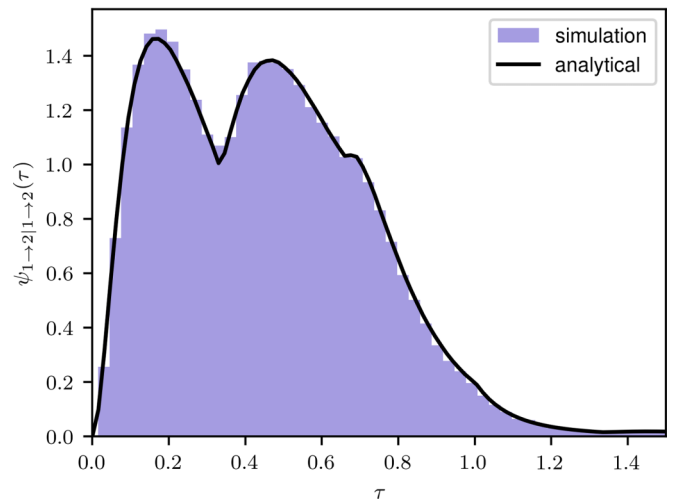$k = 10, \ F = 2, \ F_e = 1, \ B = 1.5$

FIG. 6. Comparison between analytical method and numerics for the intertransition time distribution $\psi_{\ell'|\ell}(\tau)$ for the three-state model. The transitions are $\ell = \ell' = 12$.

t_0. If the transition $\ell = i \to j$, then the initial state of the auxiliary process is j, i.e., the initial probability density of the auxiliary process $Q_a^{\text{ini}}(t_0)$ is a delta function that is one only for the state corresponding to j and zero otherwise. Hence, we obtain $\mathcal{P}_{\ell', \tau + t_0 | \ell, t_0} = \partial_\tau Q_a(\tau + t_0)$, where the state a is the absorbing state corresponding to the transition ℓ' and

$$Q_a(\tau + t_0) = \sum_b \left[\mathcal{T} \left\{ \exp \int_{t_0}^{\tau + t_0} ds \mathbf{W}_{\text{aux}}(s) \right\} \right]_{b,a} Q_b^{\text{ini}}(t_0). \tag{32}$$

The intertransition time distribution $\psi_{\ell' | \ell}(\tau)$ can be calculated by evaluating $Q_a(\tau + t_0)$ from the above equation for all $t_0 \in [0, T]$, taking its derivative and then applying Eq. (11). In Fig. 6, we show the agreement between the intertransition time distribution obtained analytically from this method and numerically from a single trajectory.

VI. CONCLUSION

We proposed a method for the inference of entropy production from the statistics of the intertransition times of a few visible transitions in periodically driven systems. If sufficient data is available, the estimator $\sigma_{\mathcal{L}}$, which depends on both the intertransition time and the initial time of the first transition estimator, provides the tightest bound to the rate of entropy production. The more accessible estimator $\hat{\sigma}$ is obtained by eliminating the need to track the initial time. It is related to the rate of entropy production σ with a formal inequality that requires the extra term X. While our numerics indicate the possibility of the inequality $\sigma \geqslant \hat{\sigma}$, this result remains restricted to our case study. The formal inequality we obtained here is $\sigma \geqslant \hat{\sigma} - X$. The emergence of this extra term and the necessity to generate two trajectories, one with forward protocol and another with backward protocol, are two main differences between the inference of entropy production for steady states and periodically driven systems.

We applied our estimators to a simple three-state model for a molecular pump leading to two general lessons. First, even in a unicyclic system, the estimate does not equal the exact rate of entropy production. This result shows a key difference in relation to steady states, for which the estimate does equal the exact entropy production in unicyclic systems [42,43]. Second, the emergence of a net current in periodically driven systems, which is not a necessary condition for a nonzero entropy production, seems to be a necessary condition for

$\hat{\sigma}$ to provide a meaningful estimate of the rate of entropy production. We observed that when the net current is zero the estimate is often numerically compatible with zero and does not capture any information about the real rate of entropy production. It would be interesting to investigate in which regimes the estimator $\hat{\sigma}$ is exactly zero, for instance in the case of no pumping. For cases with an emergent current, such as a molecular pump with a nonzero energy barrier or for a nonzero thermodynamic affinity, the method can provide a good estimate of the rate of entropy production. Hence, the method we propose here is a good candidate to estimate the rate of entropy production in physical systems with a nonzero net current such as molecular pumps and should not give much information for systems with a zero net current, such as heat engines.

A recent independent study [64] on the same topic of inference of entropy production in periodically driven systems came to our knowledge after we completed this work. Their approach is complementary to ours: They propose an estimator based on intertransition time statistics similar to $\hat{\sigma}$, in the form of a numerical conjecture, that has the advantage of only depending on statistics associated with the forward trajectory. Our work shows that, at the expense of running trajectories with the reverse protocol, a formal inequality between the estimator, extra term X, and real rate of entropy production can be proven. Moreover, it would be interesting to compare the performance of our present bounds with the bound for periodically driven systems associated with the thermodynamic uncertainty relation from [41], which depends on a single current. Such a comparison can be meaningful if the visible transitions are the ones related to a single current.

From a mathematical perspective, it would be interesting to prove whether the inequality $\sigma \geqslant \hat{\sigma}$, observed to hold within our numerics, is indeed correct. Interesting directions for future work include the study of inference of entropy production for the case of cyclic stochastic protocols, the investigation of other methods that do not require access to a trajectory with backward protocol, and a rigorous classification of physical systems for which the method can provide a good estimate.

[1] C. Jarzynski, Annu. Rev. Condens. Matter Phys. **2**, 329 (2011).

[2] U. Seifert, Rep. Prog. Phys. **75**, 126001 (2012).

[3] C. V. den Broeck and M. Esposito, Physica A **418**, 6 (2015).

[4] S. Ciliberto, Phys. Rev. X **7**, 021051 (2017).

[5] D. Collin, F. Ritort, C. Jarzynski, S. B. Smith, I. Tinoco Jr., and C. Bustamante, Nature (London) **437**, 231 (2005).

[6] V. Blickle, J. Mehl, and C. Bechinger, Phys. Rev. E **79**, 060104(R) (2009).

[7] A. Bérut, A. Arakelyan, A. Petrosyan, S. Ciliberto, R. Dillenschneider, and E. Lutz, Nature (London) **483**, 187 (2012).

[8] J. V. Koski, V. F. Maisi, T. Sagawa, and J. P. Pekola, Phys. Rev. Lett. **113**, 030601 (2014).

[9] E. Dieterich, J. Camunas-Soler, M. Ribezzi-Crivellari, U. Seifert, and F. Ritort, Nat. Phys. **11**, 971 (2015).

[10] A. Kumari, P. S. Pal, A. Saha, and S. Lahiri, Phys. Rev. E **101**, 032109 (2020).

[11] A. C. Barato and U. Seifert, Phys. Rev. Lett. **114**, 158101 (2015).

[12] T. R. Gingrich, J. M. Horowitz, N. Perunov, and J. L. England, Phys. Rev. Lett. **116**, 120601 (2016).

[13] P. Pietzonka, A. C. Barato, and U. Seifert, Phys. Rev. E **93**, 052145 (2016).

[14] A. C. Barato and U. Seifert, J. Phys. Chem. B **119**, 6555 (2015).

[15] P. Pietzonka, A. C. Barato, and U. Seifert, J. Stat. Mech. (2016) 124004.

[16] P. Pietzonka, F. Ritort, and U. Seifert, Phys. Rev. E **96**, 012101 (2017).

[17] J. Li, J. M. Horowitz, T. R. Gingrich, and N. Fakhri, Nat. Commun. **10**, 1666 (2019).

[18] T. Van Vu, V. T. Vo, and Y. Hasegawa, Phys. Rev. E **101**, 042138 (2020).

[19] A. Dechant and S.-i. Sasa, Phys. Rev. X **11**, 041061 (2021).

[20] E. Roldán and J. M. R. Parrondo, Phys. Rev. Lett. **105**, 150607 (2010).

[21] E. Roldán and J. M. R. Parrondo, Phys. Rev. E **85**, 031129 (2012).

[22] S. Muy, A. Kundu, and D. Lacoste, J. Chem. Phys. **139**, 124109 (2013).

[23] I. A. Martínez, G. Bisker, J. M. Horowitz, and J. M. Parrondo, Nat. Commun. **10**, 3542 (2019).

[24] J. Ehrich, J. Stat. Mech. (2021) 083214.

[25] D. J. Skinner and J. Dunkel, PNAS **118**, e2024300118 (2021)

[26] D. J. Skinner and J. Dunkel, Phys. Rev. Lett. **127**, 198101 (2021).

[27] S. Rahav and C. Jarzynski, J. Stat. Mech.: Theor. Exp. (2007) P09012.

[28] A. Puglisi, S. Pigolotti, L. Rondoni, and A. Vulpiani, J. Stat. Mech. (2010) P05015.

[29] M. Esposito, Phys. Rev. E **85**, 041125 (2012).

[30] J. Mehl, B. Lander, C. Bechinger, V. Blickle, and U. Seifert, Phys. Rev. Lett. **108**, 220601 (2012).

[31] S. Bo and A. Celani, J. Stat. Phys. **154**, 1325 (2014).

[32] F. Knoch and T. Speck, New J. Phys. **17**, 115004 (2015).

[33] N. Shiraishi and T. Sagawa, Phys. Rev. E **91**, 012130 (2015).

[34] G. Bisker, M. Polettini, T. R. Gingrich, and J. M. Horowitz, J. Stat. Mech. (2017) 093210.

[35] D. Seiferth, P. Sollich, and S. Klumpp, Phys. Rev. E **102**, 062149 (2020).

[36] G. Teza and A. L. Stella, Phys. Rev. Lett. **125**, 110601 (2020).

[37] J. Degünther, J. van der Meer, and U. Seifert, Proc. Natl. Acad. Sci. USA **121**, e2405371121 (2024).

[38] P. Singh and K. Proesmans, Commun. Phys. **7**, 231 (2024).

[39] S. Lee, D.-K. Kim, J.-M. Park, W. K. Kim, H. Park, and J. S. Lee, Phys. Rev. Res. **5**, 013194 (2023).

[40] S. Otsubo, S. K. Manikandan, T. Sagawa, and S. Krishnamurthy, Commun. Phys. **5**, 11 (2022).

[41] T. Koyuk and U. Seifert, Phys. Rev. Lett. **125**, 260604 (2020).

[42] J. van der Meer, B. Ertel, and U. Seifert, Phys. Rev. X **12**, 031025 (2022).

[43] P. E. Harunari, A. Dutta, M. Polettini, and E. Roldán, Phys. Rev. X **12**, 041026 (2022).

[44] T. Schmiedl and U. Seifert, Europhys. Lett. **81**, 20003 (2008).

[45] V. Blickle and C. Bechinger, Nat. Phys. **8**, 143 (2012).

[46] K. Brandner, K. Saito, and U. Seifert, Phys. Rev. X **5**, 031019 (2015).

[47] I. A. Martinez, E. Roldán, L. Dinis, and R. A. Rica, Soft Matter **13**, 22 (2017).

[48] S. Krishnamurthy, S. Ghosh, D. Chatterji, R. Ganapathy, and A. Sood, Nat. Phys. **12**, 1134 (2016).

[49] A. Datta, P. Pietzonka, and A. C. Barato, Phys. Rev. X **12**, 031034 (2022).

[50] S. Rahav, J. Horowitz, and C. Jarzynski, Phys. Rev. Lett. **101**, 140602 (2008).

[51] V. Y. Chernyak and N. A. Sinitsyn, Phys. Rev. Lett. **101**, 160601 (2008).

[52] C. Maes, K. Netocný, and S. R. Thomas, J Chem. Phys. **132**, 234116 (2010).

[53] S. Rahav, J. Stat. Mech. (2011) P09020.

[54] D. Mandal, Europhys. Lett. **108**, 50001 (2014).

[55] G. Verley, C. Van den Broeck, and M. Esposito, New J. Phys. **16**, 095001 (2014).

[56] S. Asban and S. Rahav, Phys. Rev. Lett. **112**, 050601 (2014).

[57] R. D. Astumian, Phys. Rev. Lett. **101**, 046802 (2008).

[58] S. Erbas-Cakmak, D. A. Leigh, C. T. McTernan, and A. L. Nussbaumer, Chem. Rev. **115**, 10081 (2015).

[59] O. Raz, Y. Subaşi, and C. Jarzynski, Phys. Rev. X **6**, 021022 (2016).

[60] A. C. Barato and U. Seifert, Phys. Rev. X **6**, 041053 (2016).

[61] S. Ray and A. C. Barato, Phys. Rev. E **96**, 052120 (2017).

[62] K. Sekimoto, arxiv:2110.02216.

[63] A. C. Barato and R. Chetrite, J. Stat. Mech. (2018) 053207.

[64] A. M. Maier, J. Degünther, J. van der Meer, and U. Seifert, J. Stat. Phys. **191**, 104 (2024).